Loss of CO 2 from Monodeprotonated Phthalic Acid upon Photodissociation and Dissociative Electron Detachment

Ernesto Marceca, Jennifer A. Noble, Claude Dedonder-Lardeux, Christophe Jouvet

Loss of CO_2 from Monodeprotonated Phthalic Acid upon Photodissociation and Dissociative Electron Detachment

Ernesto Marceca[1], Jennifer A. Noble[2*], Claude Dedonder-Lardeux[2] and Christophe Jouvet[2]

1: INQUIMAE (CONICET – Universidad de Buenos Aires), DQIAQF (Facultad de Ciencias Exactas y Naturales, Universidad de Buenos Aires, Ciudad Universitaria), 3er piso, Pab. II, 1428 Buenos Aires, Argentina.
2: CNRS, Aix Marseille Univ., PIIM, Marseille, France. *jennifer.noble@univ-amu.fr

Abstract

The decarboxylation (CO_2 loss) mechanism of cold monodeprotonated phthalic acid was studied in a photodissociation action spectrometer by quantifying mass-selected product anions and neutral particles as a function of the excitation energy. The analysis proceeded by interpreting the translational energy distribution of the generated uncharged products, and with the help of quantum calculations. In particular, this study reveals different fragmentation pathways in the deprotonated anion and in the radical generated upon electron photodetachment. Unlike the behaviour found in other deprotonated aryl carboxylic acids, which do not fragment in the anion excited state, a double loss of CO_2 molecules takes place in the phthalic monoanion. Moreover, at higher excitation energies the phthalic monoanion experiences decarboxylative photodetachment with a statistical distribution of product translational energies, which contrasts with the impulsive dissociation reactions characteristic of other aryl carboxylic anions.

Introduction

Decarboxylation (loss of CO_2) of carboxylic acids plays an important role in organic synthesis due to the high potential of attaining versatile decarboxylative functionalization reactions, including the generation of new carbon skeletons by coupling the structure of the acid to other substrates.[1] In the case of alkyl carboxylic acids, the -COOH group can be easily removed from the acid, e.g. by photoredox catalysis, and this activation process can later be used in combination with other catalytic functionalization steps in a solvent-based synthesis.[2,3] The process is normally initiated by the formation of an active R-COO$^\bullet$ radical intermediate, which rapidly eliminates CO_2 to give the corresponding alkyl radical (R$^\bullet$) involved in further transformations. However, for aromatic carboxylic acids –e.g. substituted benzoic acids– it was observed that under mild conditions the Ar-COO$^\bullet$ radical does not proceed with the decarboxylation step,[4,5] and loss of CO_2 only occurs under more demanding conditions or when sophisticated chemical strategies are applied.[6]

The CO_2 loss mechanism in aryl carboxylic acids can also be investigated using cold molecules in the gas phase, along a reaction coordinate that comprises either a deprotonated anion

(vibrationally or electronically excited) or the corresponding radical species formed after electron detachment. In the first case, a straightforward experimental approach consists of applying ion beam, trapping and mass selection/detection techniques to the study of the conjugate form of a carboxylic acid (Ar-COO^- anion), which can easily be generated in an electrospray source in negative-ion mode. Using this experimental platform, it was shown that infrared multiple photon excitation of $C_6H_5COO^-$ opens a ($C_6H_5^-$ + CO_2) fragmentation channel, which provides spectroscopic information on the precursor anion by plotting the product ion yield vs. the excitation wavelength.[7] In addition, collision activated dissociation studies performed on several substituted aryl carboxylic anions have also revealed loss of CO_2 molecules.[8,9] However, UV electronic excitation of deprotonated benzoic acid proved to be totally inefficient to induce fragmentation of the anion, and the molecular anion remained intact.[10] Remarkably, the opposite happens for the deprotonated naphthoic acid homologue, which exhibits decarboxylative fragmentation due to the opening of a new low-energy channel involving internal conversion and dissociation in the ground state. Further work is still required to establish how the presence of additional functional groups on the aromatic skeleton of aryl carboxylic anions will affect the elimination of CO_2 molecules.

It is well known that small molecular anionic systems can undergo a second type of dissociation process induced by UV excitation, in which the system is vertically placed on the reaction coordinate of the neutral radical species generated by electron detachment.[11] For example, dissociative photodetachment of cold deprotonated acetic acid (CH_3COO^-) has been studied using photoelectron-photofragment coincidence spectroscopy, giving a complete description of the ($CH_3COO^\bullet \rightarrow CH_3^\bullet + CO_2$) rearrangement reaction.[12] The dissociative photodetachment mechanism has also been described in deprotonated aryl carboxylic acids, such as benzoic or naphthoic anions, by measurement of the kinetic energy of the neutral species involved in the reaction, that is the remaining unfragmented radical ($C_6H_5COO^\bullet$ or $C_{10}H_7COO^\bullet$) together with the respective photoproducts ($C_6H_5^\bullet + CO_2$) or ($C_{10}H_7^\bullet + CO_2$).[10] For these two systems, low energy dissociation barriers could be determined along the C-$COO^\bullet$ bond, which rapidly rearranges by elimination of a CO_2 molecule. The loss of CO_2 from isolated $C_6H_5COO^\bullet$ contrasts with the relatively high stability shown by this radical in solution, as mentioned earlier.

The dissociative mechanism involving odd-electron species can, in principle, compete with the anionic photodissociation process. This happens in cases with optical access to an anionic excited state (with a significant oscillator strength) in the same energy range as the adiabatic detachment energy (ADE), as shown previously for the green fluorescent protein chromophore.[13,14] The dissociation yield on the radical potential energy surface becomes active at high energies, once the photodetachment channel opens, while dissociation in the anion excited state only predominates if the energy onset of the electronic transition is low and well separated from the ADE. Using this argument, it is possible to explain the lack of anionic photodissociation observed for $C_6H_5COO^-$, and the existence of competing ($C_{10}H_7^\bullet + CO_2 + e^-$) and ($C_{10}H_7^- + CO_2$) routes found for $C_{10}H_7COO^-$, since the extended π-system in the latter will shift the absorption to lower energies and hence increase the contribution of anionic dissociation.

A question arises about the response of an aryl dicarboxylic acid upon photodissociation. The monoanionic form (monodeprotonated) is of higher interest because it is the major species produced in the electrospray source operated under typical conditions. The presence of a second carboxylic group in the aryl structure alters the excitation energy profile of the anion,[15] and it is

likely to change the fragmentation dynamics as well. In the case of symmetrical vicinal dicarboxylic monoanions (ortho isomers), there is an additional topic of interest concerning the location of the hydrogen atom in the intramolecular H-bond that is established between the two (equivalent) carboxylic groups.[16] A representative model system to study the symmetry of such an intramolecular H-bond is the monodeprotonated phthalic acid (HPA^-, that may also be referred to as benzenedicarboxylic monoanion). In the gas phase, the intramolecular H-bond in HPA^- is symmetric and hence the negative charge is equally delocalised over the two carboxylic groups.[17] In this work, we investigated whether single and/or double elimination of CO_2 molecules from monodeprotonated phthalic acid can be induced by UV dissociation in the anionic state or by dissociative detachment in the radical state. Spectroscopic studies on HPA^- were done by collecting the fragmentation yield of ions and neutrals as a function of the excitation energy. We made a comparative analysis of the results with those obtained earlier for monodeprotonated benzoic and naphthoic acids,[10] with a focus on identifying the opening of new fragmentation channels in HPA^- and, eventually, describing the presence of a barrier along the CO_2 loss reaction coordinate. The experiments were interpreted with the aid of quantum calculations.

Methods

Experimental:

We have developed a new method to characterise the excited state dynamics of cold negative molecular ions. The experimental setup is essentially a cryogenic ion trap-based photodissociation action spectrometer adapted to work with negatively charged particles, with the possibility to detect and quantify both product ions and neutrals. A detailed description of the apparatus is already available in former publications.[18–20]
Photodissociation action spectroscopy is widely used to determine the photophysical properties of isolated molecular ions.[21–27] The action signal, usually originating from photodissociation or electron photodetachment events, can easily be assessed by collecting and measuring the yield of product particles as a function of the excitation energy. In absence of an active fluorescence channel, the action spectrum becomes a means to determine the absorption spectrum.

HPA^- monoanions are generated in an electrospray source (ESI) set in negative mode operation, by injecting a 10^{-4} M solution of phthalic acid dissolved in a 5:1 methanol-water mixture. The ions arrive at the trap just after a helium gas pulse and remain stored for a few tens of milliseconds, the time required to pump down the pressure in the trap and cool down the ion temperature to 30 K by collisions.[28] Next, the cold ions are extracted from the trap, accelerated to 2600 V, and focussed in the centre of a Gauss tube set at the same potential. Before the ions leave the Gauss tube, they are referenced to ground potential and finally enter a 1 m long flight tube of a linear mass spectrometer that ends in a microchannel detector.[29]
Excitation of molecular anions is done by use of a tuneable OPO laser (EKSPLA, 10 Hz repetition rate, 10 ns pulse width, 10 cm^{-1} spectral resolution, and linear polarization perpendicular to the anion displacement). The laser is focused with a 1 m focal lens and the power is typically between 0.1 and 0.5 mJ/pulse. The spectra are corrected for the laser intensity variation.
Product anions and neutrals formed on a dissociative excited S_n state energy surface (or in the hot ground state after internal conversion), can be monitored in our apparatus as a function of the excitation wavelength. In addition to the de-excitation channel in the excited state, direct or

dissociative electron detachment mechanisms can also be active, producing parent and/or product neutrals that give rise to a measurable overall signal of uncharged particles. Since particle intensity, either anionic or neutral, is proportional to the amount of light absorbed, two types of experiments can be carried out with our apparatus:

i. Mass-selected anion yield vs. excitation energy spectrum (detection of product ions). In this configuration, the anions are excited inside the cold trap. Immediately after the laser shot, the ion content of the trap (remaining precursor and product anions) are extracted, mass selected and quantified in different mass channels. If the excited state is dissociative, a fragmentation reaction takes place.
ii. Neutral particle yield vs. excitation energy spectrum (detection of neutrals). In this mode, the anions interact with the laser inside the Gauss tube, where they may experience electron detachment and eventually fragment. A deceleration potential at the exit of the tube guarantees that only neutral particles – the unfragmented precursor radical and smaller dissociation products – continue their flight towards the detector. Valuable information can be gained from the temporal profile of the signal of uncharged particles. Since dissociation is triggered by pulsed excitation, the time of flight (TOF) distribution provides a measure of the released translational energy of the two expanding fragments,[30] which in turn sheds light on the stability of the precursor radical. For certain systems, TOF peak shape analysis as a function of the excitation energy provides experimental access to the value of the adiabatic detachment energy threshold.[10,20]

Before stepping the wavelength, the signal is averaged over 8 laser shots, and the whole spectral measurement is repeated and averaged a few times, according to the intensity and the stability of the source. Temporal windows can be implemented to sample the TOF peak of neutral particles, either at the centre (unfragmented radical contribution) or at the wings (dissociation products). The TOF distribution that characterises the signal of uncharged particles is symmetrised by using the procedure explained in recent publications.[10,19,20] No smoothing algorithms were applied to the data, and the observed noise results principally from the source instability and the statistical uncertainty of the measure.

Calculations:

Adiabatic and vertical detachment energies (ADE and VDE, respectively), unimolecular dissociation energies in the HPA^- and $HPA^\bullet$ coordinates, as well as $S_n \leftarrow S_0$ vertical excitation energies and oscillator strengths were calculated at the DFT/CAM-B3Lyp/aug-cc-pVDZ level to assist the interpretation of the experimental results. The calculations were performed using Gaussian 09.[31] It should be noted that the calculations do not account for the extension of the vibrational wavefunction and tunnelling along the O—H—O coordinate of the intramolecular hydrogen bond present in the phthalic monoanion.

Results and Discussion

Scope of the experimental method:

As mentioned earlier, the TOF peak shape for neutral particles is a signature of the dissociation mechanisms taking place as a result of the excitation. We have identified at least six distinctive expected scenarios that differentiate the photodissociation mechanism that has taken place for a certain system, and we provide in Fig. 1 examples of most of these situations measured with our setup in the neutral particle detection mode. TOF peaks of neutrals can adopt the following characteristics shapes:

a) Symmetric exponential decrease of the signal: this denotes the occurrence of a reaction with a statistical product energy distribution, originating in a thermal sample of a neutral or anionic precursor. It is the case of a dissociation process in the excited state of the anion leading to one ionic fragment and one neutral fragment. An example of this situation is the observed peak of the naphthoyloxy radical (Fig. 1a) generated upon excitation at lower energies than the anion's ADE.[10] In this situation, electron detachment is unavailable, and the dissociation reaction occurs in the S_n excited state of the deprotonated anion.
b) TOF signal as narrow as the resolution of the spectrometer: it represents a non-dissociative process. The signal is due to the presence of stable radicals generated after electron photodetachment from the anion. No fragmentation occurs in the anion excited state nor in the neutral radical. Such behaviour was found in deprotonated indole at all energies above the ADE, the excitation of the anion leading to the stable indolyl radical (Fig. 1b).[32]
c) A combination of the two preceding situations: in this case, photodissociation in the anionic excited state occurs together with photodetachment. Both competitive channels can be open when the lower lying anionic excited states of the system are energetically close to the ADE. We have found this situation by exciting deprotonated *p*-toluenesulfonic acid at 260 nm (Fig. 1c).[19] Here, a statistical product energy distribution is observed at the base of the signal, accounting for a fragmentation process in the anion excited state, which is superimposed upon a narrow central component that results from a non-dissociative electron detachment event.
d) Two squared functions convolved with the apparatus function, with no sign of a central narrow peak: such an observation implies that the kinetic (translational) energy released is split into two quasi-isotropic distributions (impulsive KER), which likely indicates the presence of a dissociative detachment process. This happens when, for example, an unstable radical suffers an impulsive dissociation leading to two neutral fragments. We have observed this pattern for phenylalanine upon excitation at 235 nm, above the photodetachment threshold (Fig. 1d).[20] The two broad components of the peak are accounted for by the ($C_9H_{10}NO_2^- \rightarrow C_8H_{10}N^\bullet + CO_2 + e^-$) dissociation reaction, ascribing the one with a wider kinetic energy dispersion to the lighter CO_2 molecule, and the narrower to the complementary, heavier $C_8H_{10}N^\bullet$ fragment.
e) Two squared functions with a central narrow peak: this situation combines the scenarios b) and d), which happens when the photodetachment process leads to an internally excited radical that may or may not experience an impulsive fragmentation, i.e. only for internal energies above the dissociation barrier will the fragmentation of the radical take place. This behaviour is characteristic of deprotonated naphthoic acid upon excitation at 230 nm, above the ADE. Again, the narrow peak that emerges at the centre of the TOF profile corresponds to the unfragmented naphthoyloxy radical, while the two broad squared components are from the fragments $C_{10}H_7^\bullet$ and CO_2 resulting from the dissociative reaction.

There is another plausible TOF distribution that may be characteristic of neutrals, which has not been encountered with our method so far. It consists of simultaneous photodissociation in the anionic excited state (symmetric exponential decrease at the bottom of the signal) and an impulsive fragmentation reaction due to the radical instability (revealed as two squared components).

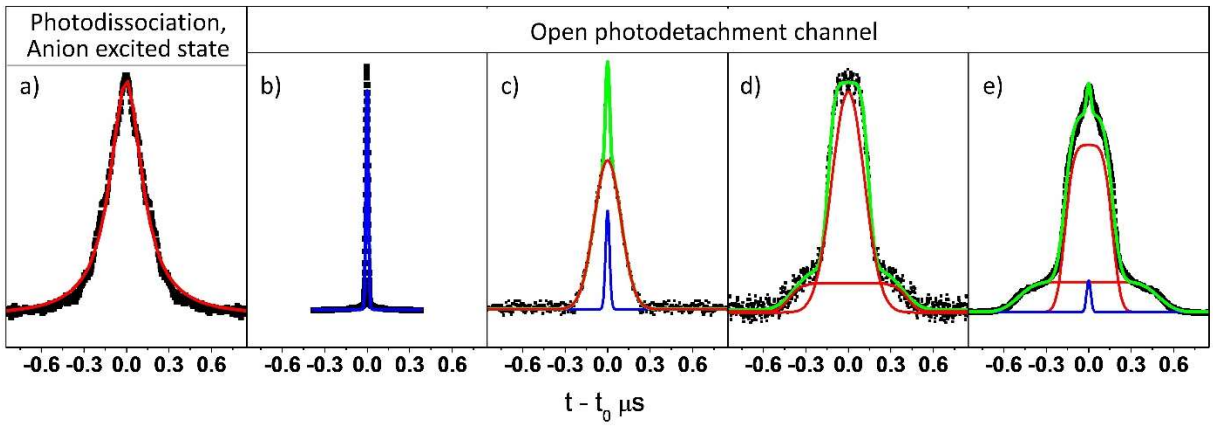

Figure 1. *Different types of TOF profiles recorded in the neutral particle detection mode for systems that release translational kinetic energy in different ways. Neutrals from fragmentation are fitted with red lines, stable radicals with blue lines, and the combined fit in green. Photoexcitation of deprotonated: a) naphthoic acid anion below the ADE - one neutral fragment, b) indole anion above the ADE - one neutral stable radical, c) p-toluenesulfonic acid anion above the ADE - two neutrals (stable radical and neutral product following anion fragmentation), d) phenylalanine anion above the ADE - two neutral fragments, and e) naphthoic acid anion above the ADE - three neutrals (stable radical and two neutral fragments).*

Action spectra of Monodeprotonated Phthalic Acid:

The experimental results on HPA^- are presented in Fig. 2 and Fig. 3. Action spectra collected in both anion and neutral particle modes are shown in Fig. 2. The two spectra are similar at low excitation energies, but they differ from each other below 265 ± 1 nm (above ~4.67 eV), as the photodissociation channel in the anionic excited state becomes less favoured than photodetachment (the switch from one process to the other is indicated by an arrow in the spectrum of Fig. 2). In particular, there is a very strong absorption at ~230 nm when collecting the neutral particle yield, which is not observed by detecting the signal in the mass windows corresponding to the precursor or product anions. The same behaviour has already been observed in other deprotonated aromatic acids like sulfonic acids.[19]

The spectrum is not well resolved, and only two bands are distinguished at 284.0 nm (4.37 eV) and 275.6 nm (4.50 eV). The gas phase spectrum of monodeprotonated phthalic acid appears slightly red shifted from the corresponding aqueous solution spectrum at pH = 8, but displays the same absorption pattern.[15]

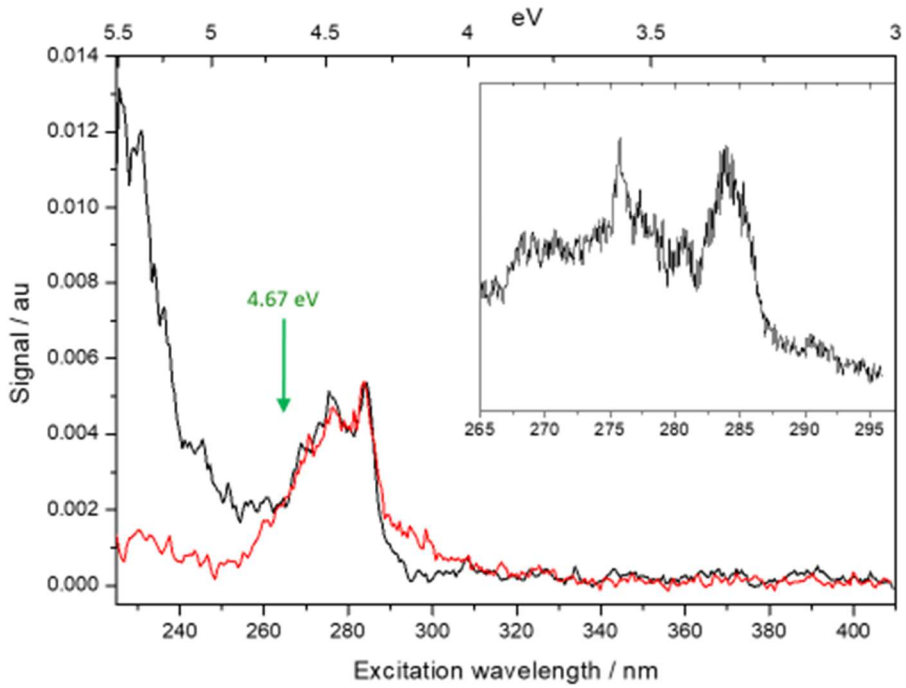

Figure 2. *Action spectra of monodeprotonated phthalic acid, collecting either the $C_6H_5^-$ anion (red) or neutral particle (black) yields as a function of the excitation energy. The arrow (located at 265 ± 1 nm) denotes the wavelength at which photodissociation and photodetachment channels switch; this value can be taken as a measure of the ADE of HPA^- (see text). The neutral particle spectrum is recorded at higher spectral resolution in the 260-300 nm range (inset).*

Unlike what we previously observed for the benzoic acid homologue,[10] HPA^- exhibits an open fragmentation channel in the anion excited state, for excitations within ~310-265 nm. Double elimination of CO_2 molecules takes place for HPA^-, which is evidenced by the appearance of a single product anion, $C_6H_5^-$, concomitant with a decrease of the precursor anion signal.

Neutral signal TOF profile:

TOF peak shapes of neutrals are shown in Fig. 3 for three excitation wavelengths, corresponding to different spectral positions: at the absorption onset (~310 nm), just above the absorption onset (295 nm), and at the strong absorption band in the mid UV region (225 nm). In all cases, the TOF profiles exhibit the same symmetric exponential decrease, with a FWHM of about 400 ns. Since anionic fragments are also measured at lower energies than the expected detachment threshold, it can be deduced that HPA^- behaves as in scenario a) described in the previous section, that is dissociation occurring in the anion excited state with a statistical product energy distribution. An additional interesting observation is that such a statistical fragmentation pattern extends to higher excitation energies, where electron photodetachment may also trigger a competitive radical based fragmentation. What is clear is that any $HPA^\bullet$ radicals formed upon photodetachment neither remain intact (lack of central narrow component in the TOF distribution) nor undergo an impulsive dissociation reaction (absence of squared components). In other words, for excitation wavelengths below ~265 nm (above ~4.67 eV), $HPA^\bullet$ radicals do not survive after photodetachment, and a second fragmentation channel opens involving other odd electron intermediates.

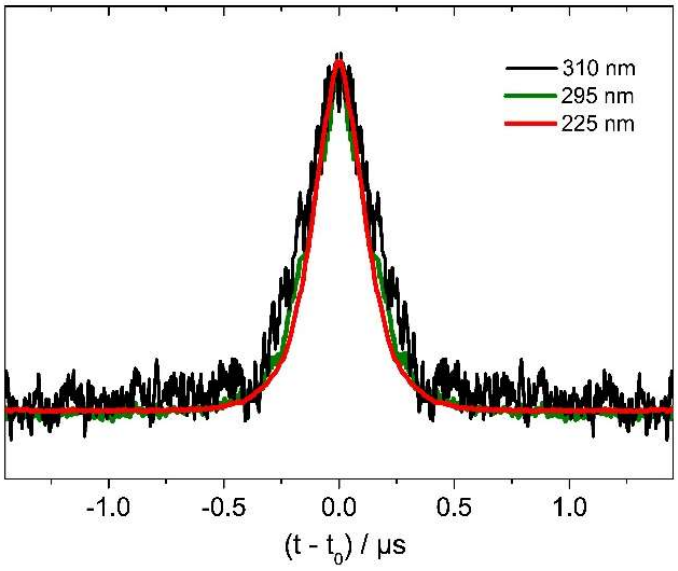

Figure 3. *Temporal profiles of the signal of neutral particles at different photon energies (FWHM ≈ 400 nm).*

Photodetachment and anionic excited state energy calculations:

In accordance with previous work on HPA^-,[16] our calculations confirmed that the ground state geometry of the monoanion is planar, with any nonplanar geometry converging towards the planar one. In the lowest energy geometry, the acidic H atom is located in the middle of two O-atoms belonging to different carboxylic groups each (see Fig. 4), forming an O···H···O Zundel-type bond with C_{2v} symmetry. Much higher in energy (1.19 eV) lies the geometry characterised by having an ordinary OH···O intramolecular hydrogen-bond, in which the H-atom is localised close to one of the oxygen atoms and where the two carboxylic groups are no longer equivalent. In view of these results, we suppose that the phthalic monoanion will adopt a Zundel-type 7-membered cyclic structure in the ground state.

According to our calculations, the $HPA^{\bullet}$ radical produced upon photodetachment of HPA^- does not dissociate. However, the Zundel-type radical accessed by vertical excitation is not a minimum energy structure. Moreover, it leads to the asymmetric OH···O form upon optimization, with a relatively large energy gain (0.80 eV lower than the Zundel-type structure). Knowing this, one can expect very different electron detachment thresholds for the anion. Indeed, this is evidenced by the large difference in the values calculated for the ADE (4.77 eV, 260.0 nm) and the VDE (5.57 eV, 222.6 nm).

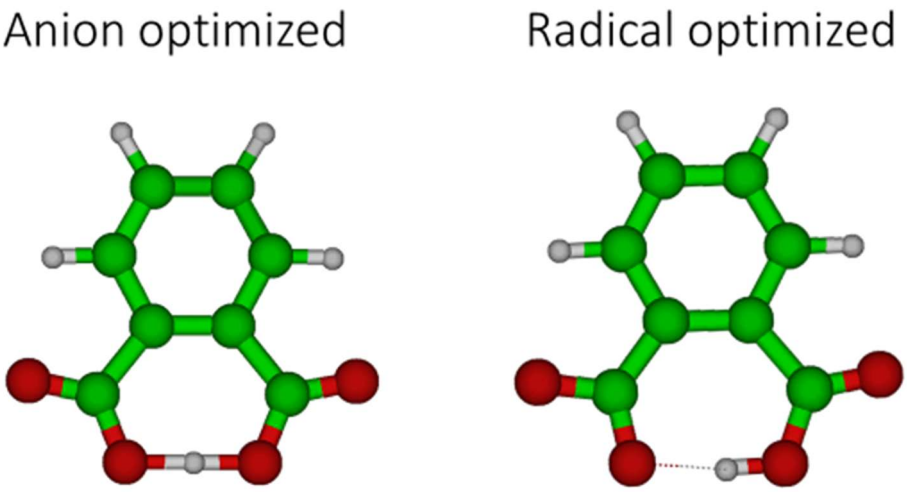

Figure 4. *Calculated optimized structures of the deprotonated monoanion (left) and of the radical (right) at the aug-cc-pVDZ/CAM-B3Lyp level. The anion has a Zundel-type structure and thus a C_{2V} symmetry; in the radical the H is localized on one of the oxygen atoms. The Cartesian coordinates are given in the SI.*

Calculated vertical excitations are given in Fig. 5. The Zundel-type structure of HPA^- exhibits only two excited states with non-zero oscillator strengths, both of which lie above 5 eV (Fig. 5, red trace). The calculated excitation states of deprotonated benzoic acid are also added in the figure for comparison (blue trace).

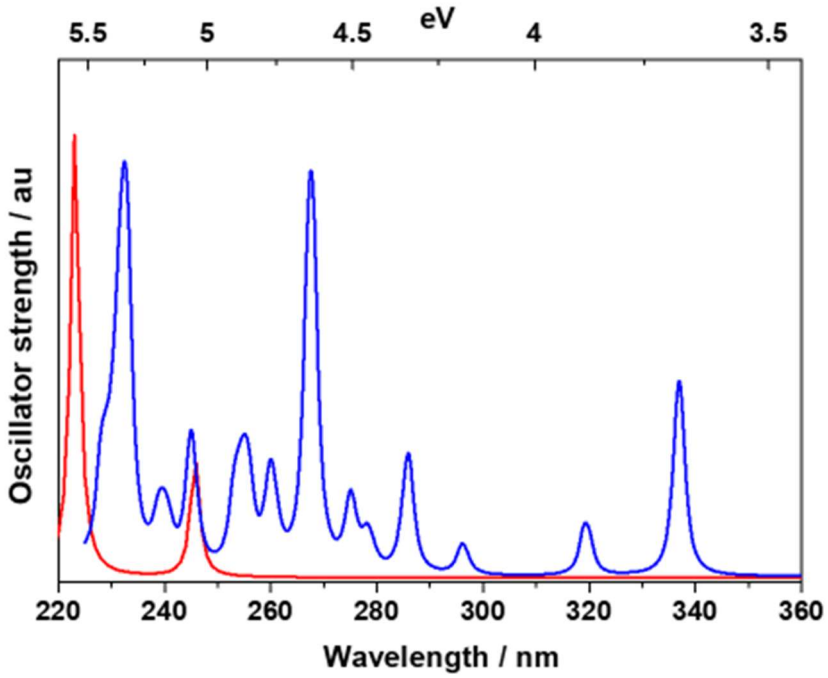

Figure 5. *Vertical excited states calculated for monodeprotonated phthalic acid for a O···H···O Zundel-type geometry (red trace). Also plotted are the calculated vertical excited states of deprotonated benzoic acid (blue trace). One should note that the calculated excited states of benzoic acid are lower in energy than those specified in ref. 10. This might be due to the use of diffuse orbitals in the basis set function of the present calculations, which should be more suitable for describing anions.*

Interpretation of the photoexcitation spectra

The calculations presented above can help in understanding the observed neutral particle and anion yield spectra. As mentioned earlier, it is quite clear from the data presented in Fig. 2 that the yield of neutrals and anions does not match for energies above 4.67 eV, a value which is very close to the calculated ADE (4.77 eV). Considering the predominance of dissociative detachment over anion fragmentation above 4.67 eV, this experimental energy threshold can be taken as a measure of the ADE. This is quite reasonable and even in quite good agreement with the calculation, owing to the uncertainty one can expect from the latter.
Moreover, it has been observed that electron detachment is a very efficient process when the photon energy is larger than the ADE. This has been observed for naphthoate,[10] as well as for aromatic phosphonate, sulfonate and phosphate oxyanions,[19] for which the differences between electron detachment and ionic fragmentation are quite easy to discriminate. For naphthoate, the radical fragments are involved in an impulsive mechanism leading to a multimodal TOF profile (Fig. 1e), with an appearance rather different to that of a statistical profile, while for phosphonate and sulfonate the radicals are stable and photodetachment leads to a narrow peak, as in Fig. 1b,c. In all these aromatic systems, a strong band at 230±10 nm (corresponding to the aromatic ring excitation) is observed, which is the one preferentially leading to the radical. The HPA^- molecular system has no reason to behave differently.

Another interpretation might be that the electron is never detached from HPA^- but, instead, the excitation is enough to break this anion into (2 CO_2 + $C_6H_5^-$), with an excess energy in the $C_6H_5^-$ fragment sufficient to remove the electron from the structure; in that case, the $C_6H_5^-$ anion signal would gradually disappear while that corresponding to the two CO_2 fragments would remain constant. This analysis would explain the shape of the observed neutral TOF signal, and hence one cannot totally exclude this possibility. However, considering that the statistical process evidenced by the TOF profiles usually reveals a distribution of internal energy, with some fragments having very little energy, one would expect that some of the $C_6H_5^-$ anions would be unable to eject an electron. Moreover, the fact that the ion signal at high energy (e.g. at 230 nm) is very weak, as compared to the neutral particle signal, would mean that nearly all the $C_6H_5^-$ fragments have a higher internal energy than the detachment threshold (and very few of them smaller internal energies), which is inconsistent with the observed statistical distribution of energy, and can occur only in direct dissociations on a repulsive potential.
Another possibility consistent with the data is the occurrence of multiphoton processes. As an example, a first photon could excite and fragment the precursor anion, and a second detach an electron from the $C_6H_5^-$ photofragment (whose EA is only 1.096 eV), either through direct photodetachment or mediated through the electronic excitation of $C_6H_5^-$. Again, although this mechanism cannot be totally excluded, there is no reason why photodetachment would occur at 250 nm and not at 280 nm, being that both energies are well above the EA. Similarly, a first photon removing an electron and a second one fragmenting the radical might also be possible. However, since the TOF profile of neutrals is apparently not consistent with a stable $HPA^\bullet$ radical (missing narrow peak), our results would only be compatible with an excitation/fragmentation yield of about 100 %, which is quite improbable.

The two bands clearly observed in the spectrum at 284 nm (4.37 eV) and 230 nm (5.29 eV) belong to excited states of the HPA^- anion. In the calculations, the first band bearing an appreciable oscillator strength corresponds to the state S_3, at 5.05 eV, and the second to the state S_5, at 5.56

eV, while the lowest S_n states are symmetry forbidden in C_{2v} symmetry. As a result, the two observed bands have been assigned to the S_3 and S_5 states. The agreement between the experiment and the calculations is not very good, but one should keep in mind that the computed values correspond to vertical excitations, which typically lower by c.a. 0.5 eV in energy upon excited state optimization and taking into consideration the change in Zero Point Energy between the ion and the radical.[33] With this in mind, the agreement between the experiment and the calculations seems reasonable, while demonstrating that calculation methods are not so good for anions or radicals despite claims to the contrary in the theoretical literature.
Unlike the benzoate anion (for which lower excited states have been calculated in the current study compared to our previous publication) these states are absent in our computations on HPA^- due to the C_{2v} symmetry of this anion, confirming that it has a Zundel-type ground state structure.

The unexpected result from these experiments is the invariant TOF profile of the neutral signal obtained for different excitation energies (shown in Fig. 3), which is indicative of the same statistical fragmentation pattern in both the anion and the radical (above 4.67 eV). From this observation we could in principle expect that fragmentation processes in both the anion and the radical are similar but, as we will demonstrate next, this is not the case.

Dissociation energies and fragmentation mechanisms:

Our initial hypothesis was that a double decarboxylation sequence occurs in both the HPA^- anion, leading to the observed photoproduct $C_6H_5^-$, as well as in the unstable $HPA^\bullet$ radical generated in the photodetachment process. Since the observed anionic photoproduct of HPA^- was $C_6H_5^-$, and since the neutral fragments would include two stable CO_2 molecules for both HPA^- and $HPA^\bullet$, this assumption seems reasonable. However, in order to assess the validity of this hypothesis, we computed the energies of plausible dissociation processes. The analysis is done bearing in mind, as discussed above, that HPA^- is most stable in its Zundel-type geometry, while the $HPA^\bullet$ radical is more energetically favourable in its asymmetric OH···O form.

In the anion, the ($HPA^- \rightarrow C_6H_5^- + 2\ CO_2$) reaction products lie 3.89 eV higher in energy than HPA^- in its Zundel-type structure. Loss of the first CO_2 molecule requires 2.24 eV, releasing 1.45 eV following $H^\bullet$ transfer to the ring to form the $C_6H_5COO^-$ anion. The loss of the second CO_2 molecule from the $C_6H_5COO^-$ anion requires an additional 3.10 eV, yielding a total reaction energy of 3.89 eV (319 nm). This energy is accessible from the observed anionic excited states, and therefore a sequential CO_2 loss is energetically allowed after internal conversion.

In the case of the $HPA^\bullet$ radical, the process that consists of a simultaneous rupture of two C-CO_2 bonds forming a benzyne biradical (as was described for the photodecomposition of gaseous phthalic anhydride)[34] and a $C_2O_4H^\bullet$ intermediate requires 3.45 eV from the optimised planar radical structure. This process is thus much too high in energy to be observed. On the other hand, a considerably lower amount of energy is calculated for the loss of 2 CO_2 ($HPA^\bullet \rightarrow C_6H_5^\bullet + 2\ CO_2$) dissociation reaction, since the reaction products lie only 0.32 eV above the stable optimized structure of the $HPA^\bullet$ radical. However, a process of this type, being endothermic, would lead to a stable $HPA^\bullet$ radical, evidencing a narrow TOF peak in the signal of neutral particles, contrary to our experimental observations. In view of that, we can conclude that the observed dissociative

electron detachment above 4.67 eV cannot lead to the same fragmentation process (loss of 2 CO_2 molecules) as that observed in the anion.

Alternatively, the energy required to lose a single CO_2 molecule from the $HPA^{\bullet}$ radical, leading to the formation of $C_6H_5COO^{\bullet}$ as counter-fragment, is exothermic. The formation of (C_6H_4COOH + CO_2) –the H atom staying on the carboxylic group– is exothermic by -0.25 eV, and the ($C_6H_5COO^{\bullet}$ + CO_2) structure obtained after H-transfer to the aromatic ring is twice as exothermic (-0.48 eV). These fragmentation reactions are found to be exothermic and can therefore occur at the threshold. However, considering that the kinetic energy released into the neutral products (TOF profile in Fig. 3) appears to have a statistical distribution, and taking into account the fact that this reaction probably requires an H-transfer from the remaining -COOH group to the ring, it is likely that a strong atomic rearrangement would be involved in the process. Such H-transfer induced rearrangement is obviously absent in the case of deprotonated benzoic acid, where a direct ($C_6H_5COO^- \rightarrow C_6H_5^{\bullet} + CO_2 + e^-$) impulsive fragmentation occurs upon photodetachment.[10]

What is interesting in the HPA^- system is the fact that the fragmentation mechanisms in the anion and in the photodetached radical are different. This is an unexpected result based upon our prior studies of carboxylic acid-bearing aromatics.

Comparison between deprotonated phthalic and other carboxylic acids:

In this section, we will summarise the differences found in the behaviour of benzoic, naphthoic and phthalic monoanions caused by photodissociation. Contrary to what it might be expected, the introduction of a second carboxylic substituent in the aromatic ring causes a marked change in the photophysics of these molecular anions. The main difference regards the dissociation in the HPA^- anion, which does not happen in the case of $C_6H_5COO^-$.

We will begin the analysis by comparing the calculated electronic states of HPA^- and $C_6H_5COO^-$ shown in Fig. 5. The overall absorption appears somewhat blue shifted for HPA^- in comparison with the $C_6H_5COO^-$ anion, with the transitions having –on average– much stronger oscillator strengths. As already mentioned in a prior section, although similar low energy excited states are calculated for the benzoate anion and for HPA^-, the latter have negligible oscillator strengths because they are forbidden in C_{2v} symmetry, confirming a Zundel-type ground state structure for HPA^-. It is quite surprising that no excited states were observed in our prior experiments on the benzoate anion (the whole spectrum was attributed to photodetachment), and this seems to indicate that when the electron detachment channel is open, electron detachment leading to the radical is faster than internal conversion leading to ionic fragmentation, which is the signature of the presence of anionic excited states. The latter argument reinforces the assignment of 3.67 eV as the threshold above which electron detachment is faster than internal conversion.

Another notable difference of HPA^- with respect to other deprotonated carboxylic homologues is the absence of a stable $HPA^{\bullet}$ radical after electron detachment. In contrast to what was found for $C_6H_5COO^{\bullet}$ and $C_{10}H_7COO^{\bullet}$ radicals, for which a marked narrow peak appears in the TOF profile of neutral particles, such a feature is absent for $HPA^{\bullet}$. This means that no late barrier of an appreciable height is able to constrain the reactivity of the $HPA^{\bullet}$ radical, and/or that the radical

obtained by electron detachment of the anionic excited state is higher in energy than the existing potential barrier. Moreover, the collected evidence indicates that the fragmentation of HPA$^{\bullet}$ does not proceed via an impulsive mechanism, as occurs for the benzoyloxy radical after surmounting a late barrier along the C-COO$^{\bullet}$ bond, but rather a single CO_2 is lost in a more complex mechanism involving H-transfer.

Conclusion

We monitored the extent of photodissociation for monodeprotonated phthalic acid in the gas phase. We registered the fragmentation spectrum by collecting both mass-selected anion and neutral particle yields as a function of the excitation wavelength, and analysed the translational energy distribution of the uncharged products generated in the UV-induced dissociation reactions. Unexpectedly, important differences arise in the photophysics of monodeprotonated phthalic, benzoic and naphthoic acids. For example, loss of CO_2 molecules takes place in the phthalic radical under statistical process, while impulsive dissociation reactions are found in the other two cases. Unfortunately, the translational energy patterns of product neutrals involved in anionic and radical dissociation processes are very similar, and hence it is not possible to definitively distinguish the ADE threshold above which HPA$^{\bullet}$ radicals are formed.

A particularly interesting result of this study is that the fragmentation pathways in the deprotonated HPA^{-} anion and in its photodetached HPA$^{\bullet}$ radical are not necessarily the same (and, indeed, they are found to be very different) for two species differing by only one electron. The question raised is as follows: is this result specific to this one case, or do the presence of multiple functional groups influence the fragmentation reactivity in other aromatic anions and radicals?

Supporting Information

The dissociation spectra of deprotonated benzoic and phthalic acid monoanions are compared, showing the yield of the different photoproducts. In addition, we provide the optimized ground state geometry and the xyz coordinates of monodeprotonated phthalic acid, in both monoanion (Zundel) and radical (non-Zundel) forms.

Acknowledgments

This work has been conducted within the International Associated Laboratory LEMIR (CNRS/CONICET) and was in part financed by the ANR Research Grant ANR2010BLANC040501-ESPEM. We also acknowledge the use of the computing facility cluster Méso-LUM of the LUMAT federation (LUMAT FR 2764). C.J. and C.D.L. would like to thank Daniel Neumark for all the fruitful and friendly discussions that we had over the course of the past thirty years.

References

(1) Gooßen, L. J.; Rodríguez, N.; Gooßen, K. Carboxylic Acids as Substrates in Homogeneous Catalysis. *Angew. Chemie - Int. Ed.* **2008**, *47*, 3100–3120.

(2) Xuan, J.; Zhang, Z.-G.; Xiao, W.-J. Visible-Light-Induced Decarboxylative Functionalization of Carboxylic Acids and Their Derivatives. *Angew. Chemie Int. Ed.* **2015**, *54*, 15632–15641.

(3) Huang, H.; Jia, K.; Chen, Y. Radical Decarboxylative Functionalizations Enabled by Dual Photoredox Catalysis. *ACS Catal.* **2016**, *6*, 4983–4988.

(4) Barton, D. H. R.; Ramesh, M. Generation and Fate of Nondecarboxylating Acyloxy Radicals Derived from the Photolysis of Acyl Derivatives of N-Hydroxy-2-Thiopyridone. *Tetrahedron Lett.* **1990**, *31*, 949–952.

(5) Hu, X.-Q.; Liu, Z.-K.; Hou, Y.-X.; Gao, Y. Single Electron Activation of Aryl Carboxylic Acids. *iScience* **2020**, *23*, 101266.

(6) Candish, L.; Freitag, M.; Gensch, T.; Glorius, F. Mild, Visible Light-Mediated Decarboxylation of Aryl Carboxylic Acids to Access Aryl Radicals. *Chem. Sci.* **2017**, *8*, 3618–3622.

(7) Steill, J. D.; Oomens, J. Action Spectroscopy of Gas-Phase Carboxylate Anions by Multiple Photon IR Electron Detachment/Attachment. *J. Phys. Chem. A* **2009**, *113*, 4941–4946.

(8) Marcum, C. L.; Jarrell, T. M.; Zhu, H.; Owen, B. C.; Haupert, L. J.; Easton, M.; Hosseinaei, O.; Bozell, J.; Nash, J. J.; Kenttämaa, H. I. A Fundamental Tandem Mass Spectrometry Study of the Collision-Activated Dissociation of Small Deprotonated Molecules Related to Lignin. *ChemSusChem* **2016**, *9*, 3513–3526.

(9) Danikiewicz, W.; Bieńkowski, T.; Poddeębniak, D. Generation and Reactions of Anionic σ-Adducts of 1,3-Dinitrobenzene and 1,3,5-Trinitrobenzene with Carbanions in a Gas Phase, Using an Electrospray Ion Source as the Chemical Reactor. *J. Am. Soc. Mass Spectrom.* **2004**, *15*, 927–933.

(10) Pino, G. A.; Jara-Toro, R. A.; Aranguren-Abrate, J. P.; Dedonder-Lardeux, C.; Jouvet, C. Dissociative Photodetachment vs. Photodissociation of Aromatic Carboxylates: The Benzoate and Naphthoate Anions. *Phys. Chem. Chem. Phys.* **2019**, *21*, 1797–1804.

(11) Continetti, R. E.; Guo, H. Dynamics of Transient Species: Via Anion Photodetachment. *Chem. Soc. Rev.* **2017**, *46*, 7650–7667.

(12) Lu, Z.; Continetti, R. E. Dynamics of the Acetyloxyl Radical Studied by Dissociative Photodetachment of the Acetate Anion †. *J. Phys. Chem. A* **2004**, *108*, 9962–9969.

(13) Nielsen, S. B.; Lapierre, A.; Andersen, J. U.; Pedersen, U. V.; Tomita, S.; Andersen, L. H. Absorption Spectrum of the Green Fluorescent Protein Chromophore Anion In Vacuo. *Phys. Rev. Lett.* **2001**, *87*, 228102.

(14) Forbes, M. W.; Jockusch, R. A. Deactivation Pathways of an Isolated Green Fluorescent Protein Model Chromophore Studied by Electronic Action Spectroscopy. *J. Am. Chem. Soc.* **2009**, *131*, 17038–17039.

(15) Guo, H.-B.; He, F.; Gu, B.; Liang, L.; Smith, J. C. Time-Dependent Density Functional Theory Assessment of UV Absorption of Benzoic Acid Derivatives. *J. Phys. Chem. A* **2012**, *116*, 11870–11879.

(16) Shenderovich, I. G. Actual Symmetry of Symmetric Molecular Adducts in the Gas Phase, Solution and in the Solid State. *Symmetry (Basel).* **2021**, *13*, 756.

(17) Garcia-Viloca, M.; González-Lafont, À.; Lluch, J. M. Asymmetry of the Hydrogen Bond of Hydrogen Phthalate Anion in Solution. A QM/MM Study. *J. Am. Chem. Soc.* **1999**, *121*,

9198–9207.
(18) Alata, I.; Bert, J.; Broquier, M.; Dedonder, C.; Feraud, G.; Grégoire, G.; Soorkia, S.; Marceca, E.; Jouvet, C. Electronic Spectra of the Protonated Indole Chromophore in the Gas Phase. *J. Phys. Chem. A* **2013**, *117*, 4420–4427.
(19) Noble, J. A.; Marceca, E.; Dedonder, C.; Carvin, I.; Gloaguen, E.; Jouvet, C. Photofragmentation and Electron Detachment of Aromatic Phosphonate, Sulfonate and Phosphate Oxyanions. *Eur. Phys. J. D* **2021**, *75*, 95.
(20) Noble, J. A.; Aranguren-Abate, J. P.; Dedonder, C.; Jouvet, C.; Pino, G. A. Photodetachment of Deprotonated Aromatic Amino Acids: Stability of the Dehydrogenated Radical Depends on the Deprotonation Site. *Phys. Chem. Chem. Phys.* **2019**, *21*, 23346–23354.
(21) Baer, T.; Dunbar, R. C. Ion Spectroscopy: Where Did It Come From; Where Is It Now; and Where Is It Going? *J. Am. Soc. Mass Spectrom.* **2010**, *21*, 681–693.
(22) Stockett, M. H.; Boesen, M.; Houmøller, J.; Brøndsted Nielsen, S. Accessing the Intrinsic Nature of Electronic Transitions from Gas-Phase Spectroscopy of Molecular Ion/Zwitterion Complexes. *Angew. Chemie Int. Ed.* **2017**, *56*, 3490–3495.
(23) Nielsen, I. B.; Boyé-Péronne, S.; El Ghazaly, M. O. A.; Kristensen, M. B.; Brøndsted Nielsen, S.; Andersen, L. H. Absorption Spectra of Photoactive Yellow Protein Chromophores in Vacuum. *Biophys. J.* **2005**, *89*, 2597–2604.
(24) Lucas, B.; Barat, M.; Fayeton, J. A.; Perot, M.; Jouvet, C.; Grégoire, G.; Brøndsted Nielsen, S. Mechanisms of Photoinduced Cα Cβ Bond Breakage in Protonated Aromatic Amino Acids. *J. Chem. Phys.* **2008**, *128*, 164302.
(25) Hanold, K. A.; Sherwood, C. R.; Continetti, R. E. Photoelectron–Neutral–Neutral Coincidence Studies of Dissociative Photodetachment. *J. Chem. Phys.* **1995**, *103*, 9876–9879.
(26) Poad, B. L. J.; Ray, A. W.; Continetti, R. E. Dissociative Photodetachment of the Ethoxide Anion and Stability of the Ethoxy Radical $CH_3CH_2O^{\bullet}$. *J. Phys. Chem. A* **2013**, *117*, 12035–12041.
(27) Faulhaber, A. E.; Szpunar, D. E.; Kautzman, K. E.; Neumark, D. M. Photodissociation Dynamics of the Ethoxy Radical Investigated by Photofragment Coincidence Imaging. *J. Phys. Chem. A* **2005**, *109*, 10239–10248.
(28) Esteves-López, N.; Dedonder-Lardeux, C.; Jouvet, C. Excited State of Protonated Benzene and Toluene. *J. Chem. Phys.* **2015**, *143*, 074303.
(29) Barat, M.; Brenot, J. C.; Fayeton, J. A.; Picard, Y. J. Absolute Detection Efficiency of a Microchannel Plate Detector for Neutral Atoms. *Rev. Sci. Instrum.* **2000**, *71*, 2050–2052.
(30) Baer, T.; Hase, W. L. *Unimolecular Reaction Dynamics*; Oxford University Press, 1996.
(31) Frisch, M. J.; Trucks, G. W.; Schlegel, H. B.; Scuseria, G. E.; Robb, M. A.; Cheeseman, J. R.; Scalmani, G.; Barone, V.; Mennucci, B.; Petersson, et al. *Gaussian 09, Revision E.01*; Gaussian, Inc., Wallingford CT, 2009.
(32) Noble, J. A.; Marceca, E.; Dedonder, C.; Jouvet, C. Influence of the N Atom and Its Position on Electron Photodetachment of Deprotonated Indole and Azaindole. *Phys. Chem. Chem. Phys.* **2020**, *22*, 27290–27299.
(33) Berdakin, M.; Féraud, G.; Dedonder-Lardeux, C.; Jouvet, C.; Pino, G. A. Excited States of Protonated DNA/RNA Bases. *Phys. Chem. Chem. Phys.* **2014**, *16*, 10643–10650.
(34) Yatsuhashi, T.; Nakashima, N. Decomposition of Gaseous Phthalic Anhydride from a Vibrationally Hot Molecule Formed by ArF Laser Irradiation. *J. Phys. Chem. A* **2000**, *104*, 203–208.

TOC Graphic